

Fixed-point iterations for several dissimilarity measure barycenters in the Gaussian case

Alessandro D’Ortenzio^{1,2}, Costanzo Manes^{1,2} and Umut Orguner³

¹Department of Information Engineering, Computer Science and Mathematics, University of L’Aquila

²Center of Excellence EX-EMERGE, University of L’Aquila

³Department of Electrical and Electronics Engineering, Middle East Technical University, Turkey

Email: alessandro.dortenzio@graduate.univaq.it^{1,2}, costanzo.manes@univaq.it^{1,2}, umut@metu.edu.tr³

Abstract—In target tracking and sensor fusion contexts it is not unusual to deal with a large number of Gaussian densities that encode the available information (multiple hypotheses), as in applications where many sensors, affected by clutter or multimodal noise, take measurements on the same scene. In such cases reduction procedures must be implemented, with the purpose of limiting the computational load. In some situations it is required to fuse all available information into a single hypothesis, and this is usually done by computing the barycenter of the set. However, such computation strongly depends on the chosen dissimilarity measure, and most often it must be performed making use of numerical methods, since in very few cases the barycenter can be computed analytically. Some issues, like the constraint on the covariance, that must be symmetric and positive definite, make it hard the numerical computation of the barycenter of a set of Gaussians. In this work, Fixed-Point Iterations (FPI) are presented for the computation of barycenters according to several dissimilarity measures, making up a useful toolbox for fusion/reduction of Gaussian sets in applications where specific dissimilarity measures are required.

Index Terms—Sensor Fusion, Gaussian densities, Fixed-point iterations.

I. INTRODUCTION

The Gaussian density is one of the most widely used model in applications, mainly because it is a reasonable approximation for many random phenomena, and it is theoretically backed by the central limit theorem. In addition, it allows for a compact and efficient way to represent uncertainties, hence resulting to be suitable for many real-time problems. Nonetheless, when dealing with several sensors, or when the uncertainty appears to be of a more complex form, it is necessary to consider sets of Gaussian components which, often, might end up being computationally intractable if not dealt with. Some examples where more than one Gaussian hypotheses appear, are target tracking in the presence of clutter, fusion of information from several sensors, stochastic switching systems, image retrieval and so on [4]. In those problems, the idea of finding a representative of a set of Gaussian densities is pursued in order to reduce the representation complexity, while preserving most of the available information. One approach to achieve this result is by computing the barycenter of a cluster of components according to a given

dissimilarity measure which, apart from very few cases where closed forms are available, might be a non-trivial task [6], [11], [12]. The outcome of such a problem strongly depends on the chosen measure, and in most cases it is necessary to resort to numerical optimization. Due to some reasons, among which the constraints on the covariance matrix, which must be symmetric and positive definite, standard optimization methods, like the gradient descent, are not well suited. A viable alternative is to consider Fixed-Point Iteration (FPI) methods which, as we will discuss in this work, provide compact recursions, very effective in evaluating the barycenter of a set of Gaussian densities.

The main goal of this work is to provide an ensemble of Fixed-Point Iterations for several dissimilarity measures that allow for the agile computation of barycenters in the Gaussian case and, in parallel, to discuss the computational issues and the barycenter features for each dissimilarity investigated. This work has been mainly motivated by the necessity to find more compact and efficient ways to evaluate barycenters in the Composite Transportation Dissimilarity Mixture Reduction framework [7], where the main bottleneck is represented by the computational load introduced by the barycenter evaluation. Nonetheless, that topic is beyond the scope of this paper, so we will limit ourselves to discuss the barycenter problem from a general perspective.

The paper is organized as follows: in Sec. II the barycenter problem is formulated; in Sec. III the problem is addressed for several dissimilarity measures, providing in parallel the corresponding fixed-point iterations. In Sec. IV a brief discussion regarding initialization of the algorithms, convergence, properties and potential links between different problems will be provided. Conclusions follow.

Notations: in this work, \mathbb{R}_+^n denotes the set of nonnegative vectors in \mathbb{R}^n , I_n is the identity matrix in $\mathbb{R}^{n \times n}$ while $\mathbf{1}_n$ denotes a vector of ones in \mathbb{R}^n . $S^d \subset \mathbb{R}^{d \times d}$ denotes the open cone of symmetric positive definite $d \times d$ matrices.

II. BARYCENTERS OF WEIGHTED SETS OF DISTRIBUTIONS

In many application domains a finite set of distributions on the same probability space is given, and there is the need of providing a single distribution that attempts to simultaneously approximate all the distributions in the set. For instance, in

This work was supported by the Centre of EXcellence on Connected, Geo-Localized and Cybersecure Vehicles (EX-EMERGE), funded by the Italian Government under CIPE resolution n. 70/2017 (Aug. 7, 2017).

applications where many sensors provide noisy measurements, modeled as probability distributions, on the same physical quantity, it may be requested to find a single distribution that is *close*, in some sense, to all the distributions provided by the sensors. This is the context of *sensor fusion*, where it is also convenient to assign nonnegative weights to the distributions in the set. The notion of barycenter of a weighted set of distributions emerges in this setting. A case of particular interest is the one where all distributions are in a given class, and the barycenter is sought in the same class [6], [11], [12]. In the case of *mixtures* of densities [4] the weights are probability masses, summing up to one. In applications, like in target tracking, where the number of mixture components exponentially grows with time and reduction procedures are needed, the computation of barycenters plays a key role [7], [13].

Consider a set of probability density functions (pdfs) $p_i(x)$, $x \in \mathbb{R}^d$, $i = 1, \dots, n$ and a set of positive weights w_i , each one associated to a distribution in the set. The set of pairs (w_i, p_i) is denoted as (\mathbf{w}, \mathbf{P}) . In particular, we will consider pdfs $p_i(x)$ in a given class \mathcal{P} of distributions.

Remark 1. *If the weights in the set sum up to 1 (i.e., $\mathbf{w}^T \mathbf{1}_n = 1$) then the combination of the distributions in \mathbf{P} with coefficients w_i , denoted $p_{\mathbf{w}, \mathbf{P}} = \sum_{i=1}^n w_i p_i$, is a convex combination, and therefore is a distribution itself, that is called a mixture of distributions in the class \mathcal{P} . Note that in general $p_{\mathbf{w}, \mathbf{P}}$ does not belong to the class \mathcal{P} .*

In order to rigorously formulate the problem of finding a distribution \hat{p} , possibly in a given class \mathcal{P} , that best approximates all the distributions in the set \mathbf{P} , possibly in the same or in another class, a measure of the *similarity* between distributions is needed to quantify how *close* or how *far* two distributions are. There are quite a lot of *dissimilarity* measures between distributions (D -measures, for short) available in the literature, often called *distorsion* measures or simply *divergences*. Some of the most used D -measures are considered in this paper, and are listed in the Appendix. The symbol $D(p||q)$ denotes a generic D -measure between two distributions p and q on the same space. In general, D -measures must satisfy the two following requirements, for all pairs of distributions p and q :

$$D(p||q) \geq 0, \quad (\text{nonnegativity}); \quad (1)$$

$$D(p||q) = 0 \iff p = q, \quad (\text{identity of indiscernibles}). \quad (2)$$

If, for any three distributions, p , q , h , the following are also satisfied

$$D(p||q) = D(q||p), \quad (\text{symmetry}); \quad (3)$$

$$D(p||q) \leq D(p||h) + D(h||q), \quad (\text{triangle inequality}), \quad (4)$$

then the dissimilarity $D(\cdot||\cdot)$ is a *distance* and defines a metric in the space of distributions. It is a very well known fact that only few D -measures considered in the literature satisfy (3) and (4). For any given D -measure that is not symmetric, it makes sense to define the *reverse* D -measure as $D^R(p||q) =$

$D(q||p)$. A list of D -measures that will be used in this paper is reported in the Appendix.

Given a weighted set of distributions (\mathbf{w}, \mathbf{P}) and a distribution p , an *Average Dissimilarity Function* (ADF) according to some chosen D -measure, can be defined as follows:

$$m_D(p|\mathbf{w}, \mathbf{P}) = \frac{1}{\mathbf{w}^T \mathbf{1}_n} \sum_{i=1}^n w_i D(p||p_i). \quad (5)$$

The barycenter \hat{p} of the weighted set (\mathbf{w}, \mathbf{P}) is defined as the distribution that minimizes the ADF (5). Mostly, we are interested in finding the barycenter in a given class \mathcal{P} of distributions, so that

$$\hat{p} = \arg \min_{p \in \mathcal{P}} m_D(p|\mathbf{w}, \mathbf{P}). \quad (6)$$

Put into words, \hat{p} is the distribution that, in average, is the *most similar* (*less dissimilar*, actually) to all distributions in the set \mathbf{P} . When the weights w_k are all equal, the barycenter is also called the *centroid* of the set [11], [12]. It is important to note that the barycenter of a set (\mathbf{w}, \mathbf{P}) strongly depends on the choice of the D -measure, as it will be discussed through the paper with some detail.

Remark 2. *Note that a different average dissimilarity may be defined by reversing the order of the distributions p_i and p in the D -measures in (5). We refer to this function of p as the reverse average dissimilarity, and denote it as m_D^R :*

$$m_D^R(p|\mathbf{w}, \mathbf{P}) = \frac{1}{\mathbf{w}^T \mathbf{1}_n} \sum_{i=1}^n w_i D(p||p_i). \quad (7)$$

Of course, the reverse average dissimilarity $m_D^R(p|\mathbf{w}, \mathbf{P})$ could be equivalently defined by using the reverse D -measure in (5), obtaining $m_D^R(p|\mathbf{w}, \mathbf{P}) = m_{D^R}(p|\mathbf{w}, \mathbf{P})$. Whenever necessary, we will refer to m_D defined in (5) as forward average dissimilarity. In the general case of non symmetric D -measures, m_D and m_D^R do not coincide, and the forward and reverse barycenters (i.e. D -barycenters and D^R -barycenters) not only do not coincide, but can be very different, as we will see in this paper.

Remark 3. *A slightly different problem can be posed When a mixture $p_{\mathbf{w}, \mathbf{P}}$ of densities in a given class \mathcal{P} is considered, instead of considering a weighted set of distributions (\mathbf{w}, \mathbf{P}) , that is the problem of approximating the mixture with a single density in the class. Note that this problem is similar, but conceptually different from the one of simultaneously approximating the single distributions in a set, and leads to the Best Single Density Approximation (BSDA) (see [7] for the Gaussian case), defined as*

$$p^* = \arg \min_{p \in \mathcal{P}} D(p_{\mathbf{w}, \mathbf{P}}||p). \quad (8)$$

Although in general the BSDA of a mixture differs from the mixture barycenter, there are few notable D -measures for which the two of them coincide.

From now on the attention will be restricted to the computation of barycenters of weighted sets of Gaussian densities.

III. BARYCENTERS OF WEIGHTED SETS OF GAUSSIANS

In this work the symbol $\mathcal{N}(x|\mu, \Sigma)$ is used to denote a multivariate non-degenerate d -dimensional Gaussian density with mean $\mu \in \mathbb{R}^d$ and covariance $\Sigma \in S^d$:

$$\mathcal{N}(x|\mu, \Sigma) = \frac{1}{\sqrt{|2\pi\Sigma|}} e^{-\frac{1}{2}(x-\mu)^T \Sigma^{-1}(x-\mu)}. \quad (9)$$

A short-hand notation for a generic Gaussian is ν , used when the mean and covariance do not need to be specified. $\mathcal{N} = \{\nu_1, \dots, \nu_n\}$ denotes a set of n Gaussians, and $(\mathbf{w}, \mathcal{N})$ denotes a Weighted Set of Gaussians (WSG). The *Average Dissimilarity Function* (ADF) of a Gaussian ν from a WSG, for a given D -measure, is defined as in (5), and conveniently rewritten as $m_D(\nu|\mathbf{w}, \mathcal{N})$. The mean and covariance of the barycenter are obtained by minimizing the ADF:

$$\begin{aligned} (\hat{\mu}, \hat{\Sigma}) &= \arg \min_{(\mu, \Sigma) \in \mathbb{R}^d \times S^d} m_D(\mathcal{N}(\cdot|\mu, \Sigma)|\mathbf{w}, \mathcal{N}) \\ &= \arg \min_{(\mu, \Sigma) \in \mathbb{R}^d \times S^d} \sum_{i=1}^n w_i D(\nu_i|\mathcal{N}(\cdot|\mu, \Sigma)), \end{aligned} \quad (10)$$

and the barycenter is $\hat{\nu} = \mathcal{N}(\cdot|\hat{\mu}, \hat{\Sigma})$ (the constant term $\mathbf{w}^T \mathbb{1}_n$ in the denominator of (5), irrelevant in the minimization, has been omitted in (10)). According to Remark 3, the *Best Single Gaussian Approximation* [7] of a mixture $p_{\mathbf{w}, \mathcal{N}} = \sum_{i=1}^n w_i \nu_i$ (Gaussian Mixture Model) is the Gaussian ν^* with minimum dissimilarity from the mixture, i.e. $\nu^* = \arg \min_{\nu} D(p_{\mathbf{w}, \mathcal{N}}|\nu)$, and in general does not coincide with the barycenter $\hat{\nu}$.

Usually, the computation of the barycenter for a weighted set of Gaussians is not an easy task: only very few D -measures admit a closed form formula for the barycenter, while in most cases the barycenter parameters $(\hat{\mu}, \hat{\Sigma})$ can only be obtained by numerically solving the constrained minimization problem (10). In these cases, algorithms like the constrained gradient descent may not be the best choice for two main reasons: 1) the computation of the gradient step while satisfying the constraint on the covariance ($\Sigma \in S^d$) is not an easy task; 2) in many cases the average dissimilarity function m_D to be minimized in (10) has many local minima, thus making the gradient algorithm rather sensitive to the initialization.

For these and other reasons, some authors started investigating the use of Fixed Point Iterations (FPI) to achieve fast and robust convergence to the barycenters [1], [6]. In this paper FPI computations of barycenters are presented for some interesting D -measures (see the list in the Appendix), together with a discussion of their features and peculiarities.

As a general approach, all FPI algorithms presented in this paper are derived by manipulating the stationary conditions obtained by setting to zero the first order derivatives of the function $m_D(\nu|\mathbf{w}, \mathcal{N})$ with respect to the parameters of the Gaussian $\nu = \mathcal{N}(x|\mu, \Sigma)$. In the derivation, the inverse of the covariance, i.e., the *precision* matrix Σ^{-1} , has been considered as a parameter, instead of the covariance Σ , because it provides simpler stationary conditions for all chosen D -measures. Indeed the partial derivatives of a Gaussian density $\nu = \mathcal{N}(x|\mu, \Sigma)$ with respect to μ and Σ^{-1} are as follows:

$$\begin{aligned} \frac{\partial \nu}{\partial \mu} &= \Sigma^{-1}(x - \mu) \cdot \nu \\ \frac{\partial \nu}{\partial \Sigma^{-1}} &= \frac{1}{2}(\Sigma - (x - \mu)(x - \mu)^T) \cdot \nu. \end{aligned} \quad (11)$$

These formulas are useful in the computations of the stationary conditions

$$\begin{aligned} \frac{\partial m_D(\nu|\mathbf{w}, \mathcal{N})}{\partial \mu} &= \frac{1}{\mathbf{w}^T \mathbb{1}_n} \sum_{i=1}^n w_i \frac{\partial D(\nu_i|\mathcal{N}(\cdot|\mu, \Sigma))}{\partial \mu} = 0 \\ \frac{\partial m_D(\nu|\mathbf{w}, \mathcal{N})}{\partial \Sigma^{-1}} &= \frac{1}{\mathbf{w}^T \mathbb{1}_n} \sum_{i=1}^n w_i \frac{\partial D(\nu_i|\mathcal{N}(\cdot|\mu, \Sigma))}{\partial \Sigma^{-1}} = 0, \end{aligned} \quad (12)$$

for specific choices of D -measures. Due to space constraints, in this paper the derivatives in (12) can not be reported for all D -measures considered.

Throughout the paper, to illustrate the features of the barycenters corresponding to different D -measures, the surface plots of the ADFs m_D over the parameter space (μ, Σ) are presented for the following simple WSG $(\mathbf{w}, \mathcal{N})$:

$$\begin{aligned} d &= 1, \quad \mathbf{w} = [0.2 \quad 0.3 \quad 0.4]^T, \\ \mu &= [-1 \quad 0 \quad 3.5]^T, \quad \Sigma = [0.05 \quad 0.1 \quad 0.15]^T. \end{aligned} \quad (13)$$

A. Forward and Reverse Kullback-Leibler Divergences

The first D -measure of the list is the celebrated *Kullback-Leibler Divergence* [10] (KLD), also known as *differential relative entropy*. Given two Gaussian densities $\nu_i = \mathcal{N}(x|\mu_i, \Sigma_i)$ and $\nu_j = \mathcal{N}(x|\mu_j, \Sigma_j)$, the KLD of ν_j from ν_i is:

$$\begin{aligned} D_{KL}(\nu_i|\nu_j) &= \int \nu_i(x) \log \frac{\nu_i(x)}{\nu_j(x)} dx \\ &= \frac{1}{2}(\text{tr}(\Sigma_j^{-1} \Sigma_i) + \log \frac{|\Sigma_j|}{|\Sigma_i|} + (\mu_j - \mu_i)^T \Sigma_j^{-1} (\mu_j - \mu_i) - d). \end{aligned} \quad (14)$$

Such divergence satisfies properties (1) and (2), but it is not symmetric, hence it makes sense to distinguish the *Forward KLD*, defined as in (14), from the *Reverse KLD*, obtained by swapping the arguments as $D_{RKL}(\nu_i|\nu_j) = D_{FKL}(\nu_j|\nu_i)$.

If the D_{FKL} is employed in (5), the system (12) admits a closed form solution that coincides with what in the literature is known as the *Moment-Preserving merge* (MP-merge) [13] of the Gaussian components. The parameters of the D_{FKL} -barycenter are as follows:

$$\hat{\mu} = \frac{1}{\mathbf{w}^T \mathbb{1}_n} \sum_{i=1}^n w_i \mu_i \triangleq \mu_{MP}, \quad (15)$$

$$\hat{\Sigma} = \frac{1}{\mathbf{w}^T \mathbb{1}_n} \sum_{i=1}^n w_i (\Sigma_i + (\mu_i - \hat{\mu})(\mu_i - \hat{\mu})^T) \triangleq \Psi_{MP}(\hat{\mu}). \quad (16)$$

Fig. 1 reports the plot of the $m_{D_{FKL}}$ surface as a function of μ and Σ for the simple set of Gaussians (13), and the location of the barycenter parameters.

Computing the D_{RKL} -barycenter, we get what in the literature is known as the *Kullback-Leibler Average* (KLA) [3] of the Gaussian components:

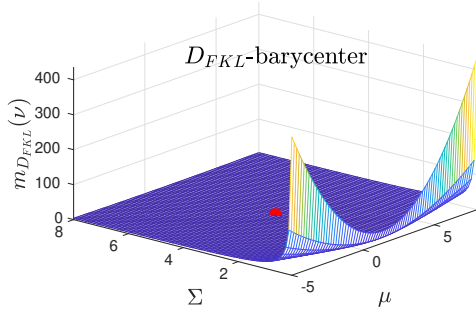


Figure 1. $\hat{\mu}_{D_{FKL}} = 1.3333$, $\hat{\Sigma}_{D_{FKL}} = 4.0000$

$$\hat{\Sigma} = \left(\frac{1}{\mathbf{w}^T \mathbf{1}_n} \sum_{i=1}^n w_i \Sigma_i^{-1} \right)^{-1} \triangleq \Psi_{KLA}, \quad (17)$$

$$\hat{\mu} = \hat{\Sigma} \left(\frac{1}{\mathbf{w}^T \mathbf{1}_n} \sum_{i=1}^n w_i \Sigma_i^{-1} \mu_i \right) \triangleq \mu_{KLA}. \quad (18)$$

For future purposes, it is also useful to define the following:

$$\tilde{\mu}_{KLA} \triangleq \frac{1}{\mathbf{w}^T \mathbf{1}_n} \sum_{i=1}^n w_i \Sigma_i^{-1} \mu_i, \quad \text{so that } \mu_{KLA} = \Psi_{KLA} \tilde{\mu}_{KLA} \quad (19)$$

The plot of $m_{D_{RKL}}$ for the example set (13) and the barycenter parameters are reported in Fig. 2. Note that the $\hat{\Sigma}_{D_{RKL}}$ is significantly smaller than the variance $\hat{\Sigma}_{D_{FKL}}$ in Fig. 1.

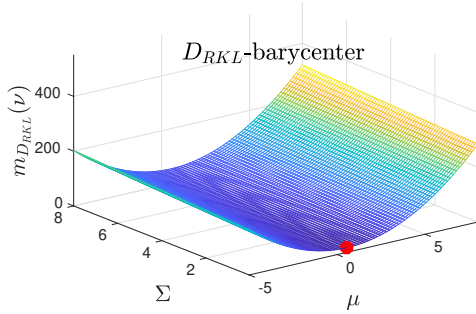


Figure 2. $\hat{\mu}_{D_{RKL}} = 0.5517$, $\hat{\Sigma}_{D_{RKL}} = 0.0931$

To the best of our knowledge, for the Gaussian case these two are the only D -measures for which the barycenter parameters can be entirely computed in a closed form. For all the other D -measures here considered, we provide fixed-point iteration (FPI) algorithms to compute the barycenter parameters.

B. Skew Jeffreys' Divergence

The Jeffreys' Divergence is a symmetrization of the KL -divergence (see the Appendix). Its skew version, also in the Appendix, depends on a parameter $\alpha \in [0, 1]$, and is applied to a pair of Gaussians ν_i and ν_j as follows:

$$D_J^\alpha(\nu_i \parallel \nu_j) = (1 - \alpha) D_{FKL}(\nu_i \parallel \nu_j) + \alpha D_{RKL}(\nu_i \parallel \nu_j), \quad (20)$$

which for $\alpha = 0.5$ recovers the symmetric Jeffreys' Divergence D_{SKL} . Using D_J^α in (12) and exploiting the formulas derived in sec. VI-A, two equations where the unknowns are the $(\hat{\mu}, \hat{\Sigma})$ parameters of the D_J^α -barycenter are obtained, not reported here due to space limitations. Such equations do not

admit a closed form solution. After some manipulations, we derived the following recursive formulas:

$$\begin{aligned} \hat{\mu}^{k+1} &= (\Gamma_{KLA}^{\alpha,k})^{-1} [\alpha \tilde{\mu}_{KLA} + (\hat{\Sigma}^k)^{-1} (1 - \alpha) \mu_{MP}] \\ \hat{\Sigma}^{k+1} &= (\Gamma_{KLA}^{\alpha,k})^{-\frac{1}{2}} ((\Gamma_{KLA}^{\alpha,k})^{\frac{1}{2}} \Gamma_{MP}^{\alpha,k} (\Gamma_{KLA}^{\alpha,k})^{\frac{1}{2}})^{-\frac{1}{2}} (\Gamma_{KLA}^{\alpha,k})^{-\frac{1}{2}} \end{aligned} \quad (21)$$

where μ_{MP} and $\tilde{\mu}_{KLA}$ are defined in (15) and (19), and

$$\begin{aligned} \Gamma_{KLA}^{\alpha,k} &= \alpha \Psi_{KLA}^{-1} + (1 - \alpha) (\hat{\Sigma}^k)^{-1} \\ \Gamma_{MP}^{\alpha,k} &= (1 - \alpha) \Psi_{MP}(\hat{\mu}^k) + \alpha \hat{\Sigma}^k. \end{aligned} \quad (22)$$

with Ψ_{KLA} defined in (17) and $\Psi_{MP}(\hat{\mu})$ defined in (16). Note that, differently from Ψ_{KLA} , the matrix Ψ_{MP} depends on the current mean $\hat{\mu}^k$, and therefore must be recomputed at each iteration. If $\alpha = 0.5$, the D_{SKL} case, the equations (21) can be simplified:

$$\begin{aligned} \hat{\mu}^{k+1} &= [\Psi_{KLA}^{-1} + (\hat{\Sigma}^k)^{-1}]^{-1} [\tilde{\mu}_{KLA} + (\hat{\Sigma}^k)^{-1} \mu_{MP}], \\ \hat{\Sigma}^{k+1} &= \Psi_{KLA}^{\frac{1}{2}} (\Psi_{KLA}^{-\frac{1}{2}} \Psi_{MP}(\hat{\mu}^k) \Psi_{KLA}^{-\frac{1}{2}})^{\frac{1}{2}} \Psi_{KLA}^{\frac{1}{2}}, \end{aligned} \quad (23)$$

which can be efficiently implemented using the Cholesky factorizations of the covariance matrices. Note that the above recursions preserve the symmetry and the positive-definiteness of the covariance matrices. As done in [1], we don't provide a proof of convergence of the iterations (21). However, an intensive campaign of numerical tests has shown nice convergence properties of the iterations. Indeed, the D_{SKL} -barycenter of a given set is unique, as proved in [12], and this justifies the nice behavior of the fixed-point recursion provided. A good choice for the initial point $(\hat{\mu}_0, \hat{\Sigma}_0)$ is the D_{FKL} -barycenter for $\alpha < 0.5$ and the D_{RKL} -barycenter for $\alpha > 0.5$. Indeed, from the definition (20), by varying $\alpha \in [0, 1]$, one can *slide* between the D_{FKL} and the D_{RKL} barycenters, passing at the D_{SKL} -barycenter for $\alpha = 0.5$. Fig. 3 reported the $m_{D_{SKL}}$ surface for the example set (13).

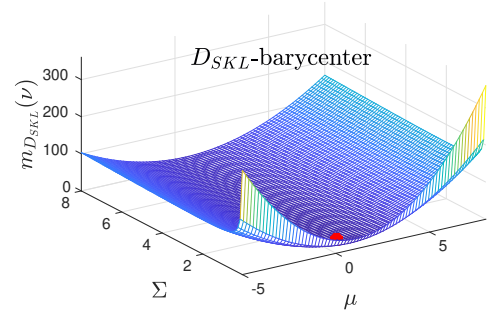


Figure 3. $\hat{\mu}_{D_{SKL}} = 0.6503$, $\hat{\Sigma}_{D_{SKL}} = 0.6449$

A discussion about the properties of the D_J^α -baricenters, which represent a trade-off between the features of the D_{FKL} and D_{RKL} barycenters, mostly in terms of *inclusiveness*, although interesting, can not be reported here due to lack of space.

C. Square 2-Wasserstein Distance

The Square 2-Wasserstein Distance (W2 for short, see the Appendix) between two Gaussian pdfs $\nu_i = \mathcal{N}(x|\mu_i, \Sigma_i)$ and $\nu_j = \mathcal{N}(x|\mu_j, \Sigma_j)$, takes the following closed form [1], [5].

$$D_{W2}(\nu_i \|\nu_j) = \|\mu_i - \mu_j\|_2^2 + \text{tr}(\Sigma_i + \Sigma_j - 2(\Sigma_i^{\frac{1}{2}} \Sigma_j \Sigma_i^{\frac{1}{2}})^{\frac{1}{2}}). \quad (24)$$

Such a D -measure is symmetric (3), and its square root is a true distance. By minimizing the average dissimilarity (10) it can be shown that the parameters of the D_{W2} -barycenter of $(\mathbf{w}, \mathcal{N})$ satisfy the following:

$$\hat{\mu} = \frac{1}{\mathbf{w}^T \mathbf{1}_n} \sum_{i=1}^n w_i \mu_i, \quad (25)$$

$$\hat{\Sigma} = \frac{1}{\mathbf{w}^T \mathbf{1}_n} \sum_{i=1}^n w_i \left(\hat{\Sigma}^{\frac{1}{2}} \Sigma_i \hat{\Sigma}^{\frac{1}{2}} \right)^{\frac{1}{2}}. \quad (26)$$

Note that the mean (25) of the D_{W2} -barycenter is the μ_{MP} (15), while (26) is a condition on the covariance that does not allow a closed form solution for $n > 2$. In [1] the uniqueness of the solution of $\hat{\Sigma}$ of (26) has been proved, and the following FPI has been proposed for its computation:

$$\hat{\Sigma}^{k+1} = \frac{1}{\mathbf{w}^T \mathbf{1}_n} \sum_{i=1}^n w_i \left((\hat{\Sigma}^k)^{\frac{1}{2}} \Sigma_i (\hat{\Sigma}^k)^{\frac{1}{2}} \right)^{\frac{1}{2}}. \quad (27)$$

Although no proof of convergence has been provided for the FPI (27) in [1], the authors claim its good convergence properties, which we have verified in our extensive numerical tests. It is interesting to note that a closed form for the D_{W2} -barycenter covariance exists for $n = 2$ [2]:

$$\hat{\Sigma} = \frac{1}{(w_i + w_j)^2} \left(w_i^2 \Sigma_i + w_j^2 \Sigma_j + w_i w_j ((\Sigma_i \Sigma_j)^{\frac{1}{2}} + (\Sigma_j \Sigma_i)^{\frac{1}{2}}) \right).$$

The plot of the $m_{D_{W2}}(\mu, \Sigma)$ for the example WSG defined in (13) is shown in Fig. 4.

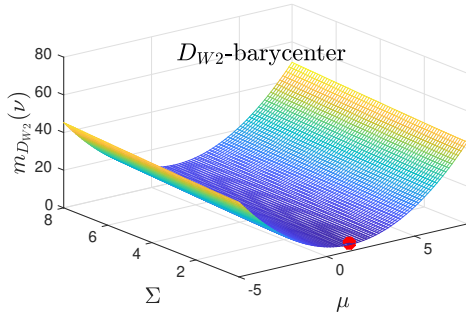


Figure 4. $\hat{\mu}_{D_{W2}} = 1.3333$, $\hat{\Sigma}_{D_{W2}} = 0.1071$

All plots reported until now show that, for the D -measures considered so far, the average divergences m_D are convex in the parameter space, thus suggesting the presence of a unique global minimizer (the barycenter). It follows that all the proposed FP iterations proposed are quite insensitive to the initialization. As we will see, though, for other D -measures this is not true anymore, and a careful initialization of the FPIs is needed to obtain the convergence to the global minimum of the m_D .

D. Likeness-based divergence family

As discussed in [9], dissimilarity measures such as the *Square L2 norm* (aka *Integral Squared Error (ISE)*) and the *Cauchy-Schwarz divergence (CSD)* (see the list in the Appendix), belong to the *Likeness-based family*. According to [9], a generic *Likeness-based D-measure* for two Gaussian pdfs ν_i and ν_j can be always put in the form:

$$D_{LB}(\nu_i \|\nu_j) = s_{LB}(J_{i,i}, J_{i,j}, J_{j,j}) \quad (28)$$

where $J_{i,i}, J_{i,j}, J_{j,j}$ are the cross- and self-likeness defined in (41) and (42), in the Appendix. that is we consider a family of D -measures which are a function of the terms (41) and (42). When searching for the D_{LB} -barycenter, the following derivatives must be computed

$$\frac{\partial D_{LB}(\nu_i \|\nu)}{\partial \theta} = c_1^{i,\nu} \frac{\partial J_{i,\nu}}{\partial \theta} + c_2^{i,\nu} \frac{\partial J_{\nu,\nu}}{\partial \theta}$$

where $\theta \in \{\mu, \Sigma^{-1}\}$, and

$$c_1^{i,\nu} = \frac{\partial s_{LB}(J_{i,i}, J_{i,\nu}, J_{\nu,\nu})}{\partial J_{i,\nu}}, \quad c_2^{i,\nu} = \frac{\partial s_{LB}(J_{i,i}, J_{i,\nu}, J_{\nu,\nu})}{\partial J_{\nu,\nu}}$$

and the likeness derivatives are reported in (50). Given a WSG $(\mathbf{w}, \mathcal{N})$ and a Gaussian ν let us define:

$$\begin{aligned} \tilde{w}_{i,\nu} &= w_i J_{i,\nu}, & \tilde{w}_{i,\nu}^{c_1} &= w_i J_{i,\nu} c_1^{i,\nu}, & \tilde{w}_{i,\nu}^{c_2} &= w_i J_{\nu,\nu} c_2^{i,\nu}, \\ \bar{w}_\nu &= \sum_{i=1}^n \tilde{w}_{i,\nu}, & \bar{w}_\nu^{c_1} &= \sum_{i=1}^n \tilde{w}_{i,\nu}^{c_1}, & \bar{w}_\nu^{c_2} &= \sum_{i=1}^n \tilde{w}_{i,\nu}^{c_2}. \end{aligned}$$

After some manipulation of the stationary equations, we derived the following general FPI algorithm for the barycenter computation in the Likeness-based family:

$$\begin{aligned} \hat{\mu}^{k+1} &= \frac{1}{\bar{w}_{\nu^k}^{c_1}} \sum_{i=1}^n \tilde{w}_{i,\nu^k}^{c_1} \bar{\mu}_{i,\nu^k}, \\ \hat{\Sigma}^{k+1} &= \frac{1}{\bar{w}_{\nu^k}^{c_1}} \left[\sum_{i=1}^n \tilde{w}_{i,\nu^k}^{c_1} (\bar{\Sigma}_{i,\nu^k} + (\bar{\mu}_{i,\nu^k} - \hat{\mu}^k)(\bar{\mu}_{i,\nu^k} - \hat{\mu}^k)^T) \right. \\ &\quad \left. - \bar{w}_{\nu^k}^{c_2} \hat{\Sigma}^k \right] \end{aligned} \quad (29)$$

where ν^k denotes the Gaussian with parameters (μ^k, Σ^k) , and $\bar{\mu}_{i,\nu^k}$ and $\bar{\Sigma}_{i,\nu^k}$ are computed as in (44). For the D_{L2} -measure, we have $c_1^{i,\nu} = -2$ and $c_2^{i,\nu} = 1$ [9], and the above recursion can be rewritten as:

$$\begin{aligned} \hat{\mu}^{k+1} &= \frac{1}{\bar{w}_{\nu^k}} \sum_{i=1}^n \tilde{w}_{i,\nu^k} \bar{\mu}_{i,\nu^k}, \\ \hat{\Sigma}^{k+1} &= \frac{1}{\bar{w}_{\nu^k}} \left[\sum_{i=1}^n \tilde{w}_{i,\nu^k} (\bar{\Sigma}_{i,\nu^k} + (\bar{\mu}_{i,\nu^k} - \hat{\mu}^k)(\bar{\mu}_{i,\nu^k} - \hat{\mu}^k)^T) \right. \\ &\quad \left. + \frac{1}{2} s(\mathbf{w}) J_{\nu^k, \nu^k} \hat{\Sigma}^k \right] \end{aligned} \quad (30)$$

where $s(\mathbf{w}) = \mathbf{w}^T \mathbf{1}_n$ Fig. 5 reports the plot of $m_{D_{L2}}$ and the barycenter parameters for the WSG example (13). Note that the $m_{D_{L2}}$ functions presents local minima, and that the global minimum is quite far from them,

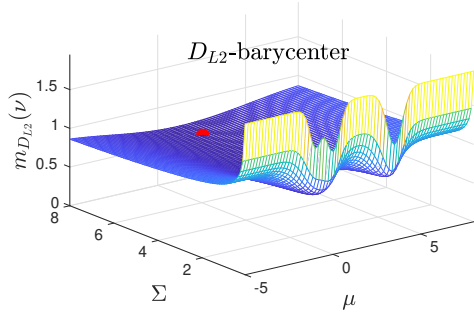


Figure 5. $\hat{\mu}_{D_{L2}} = 1.1571$, $\hat{\Sigma}_{D_{L2}} = 6.8585$

Another D -measure in the LB family we here consider is the *Cauchy-Schwarz Divergence*, for which $c_1^{i,\nu} = -\frac{1}{J_{i,\nu}}$ and $c_2^{i,\nu} = \frac{1}{2J_{\nu,\nu}}$ (see [9]). By exploiting the general form (29), we get the following recursion:

$$\begin{aligned}\hat{\mu}^{k+1} &= \frac{1}{s(\mathbf{w})} \sum_{i=1}^n w_i \bar{\mu}_{i,\nu^k}, \\ \hat{\Sigma}^{k+1} &= \frac{2}{s(\mathbf{w})} \sum_{i=1}^n w_i (\bar{\Sigma}_{i,\nu^k} + (\bar{\mu}_{i,\nu^k} - \hat{\mu}^k)(\bar{\mu}_{i,\nu^k} - \hat{\mu}^k)^T).\end{aligned}\quad (31)$$

Fig. 6 reports the plot of $m_{D_{CS}}$ and the barycenter parameters.

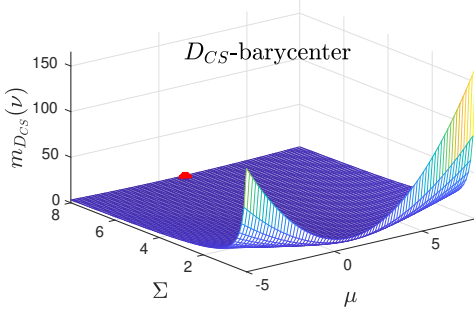


Figure 6. $\hat{\mu}_{D_{CS}} = 1.3239$, $\hat{\Sigma}_{D_{CS}} = 7.7789$

E. Chernoff α -divergences

The Chernoff α -divergences have been defined in (38)-(39) in the Appendix, for $\alpha \in (-\infty, \infty)$, and it has been shown that for some values of α they coincide with some known divergences. Here we limit ourselves to the case $\alpha \in [0, 1]$, because for $\alpha \notin [0, 1]$ the divergence is not well defined for all pairs of Gaussians.

The α -divergence of the I° kind for a pair ν_i, ν_j is

$$D_\alpha^I(\nu_i \parallel \nu_j) = \frac{1}{\alpha(1-\alpha)} (1 - c_\alpha(\nu_i, \nu_j)), \quad (32)$$

where $c_\alpha(\nu_i, \nu_j)$ is the Chernoff coefficient defined in (37), which for Gaussians takes the form (48). As done with the LB family, let us define the quantities:

$$w_{i,\nu}^{c_\alpha} = w_i c_\alpha(\nu_i, \nu), \quad \bar{w}_\nu^{c_\alpha} = \sum_{i=1}^n w_{i,\nu}^{c_\alpha}. \quad (33)$$

By using D_α^I in (5), we have been able to formulate the following FPI:

$$\hat{\mu}^{k+1} = \frac{1}{\bar{w}_\nu^{c_\alpha}} \sum_{i=1}^n w_{i,\nu^k}^{c_\alpha} \bar{\mu}_{i,\nu^k}^\alpha, \quad (34)$$

$$\hat{\Sigma}^{k+1} = \frac{1}{\bar{w}_\nu^{c_\alpha}} \sum_{i=1}^n w_{i,\nu^k}^{c_\alpha} (\bar{\Sigma}_{i,\nu^k}^\alpha + (\bar{\mu}_{i,\nu^k}^\alpha - \hat{\mu}^k)(\bar{\mu}_{i,\nu^k}^\alpha - \hat{\mu}^k)^T),$$

where $\bar{\mu}_{i,\nu^k}^\alpha$ and $\bar{\Sigma}_{i,\nu^k}^\alpha$ are defined in (49). In Fig. 7 is reported the m_D surface for $\alpha = \frac{1}{2}$, that is for the *Square Hellinger Divergence*, for the example (13).

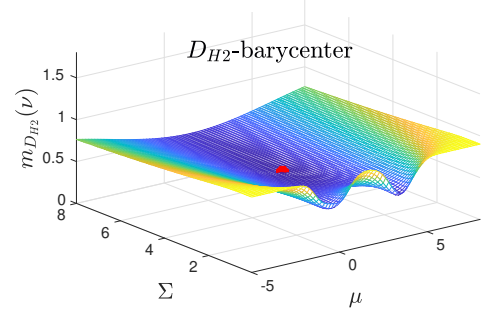


Figure 7. $\hat{\mu}_{D_{H2}} = 1.4968$, $\hat{\Sigma}_{D_{H2}} = 3.7277$

Like for the Square L2 norm, also for this class of α -divergences the function $m_{D_\alpha^I}$ may present local minima, for $\alpha \in (0, 1)$. Hence, also in this case it is important to select carefully the initial guess for the FPI. Nonetheless, for $\alpha = 0$ $D_\alpha^I = D_{RKL}$ and for $\alpha = 1$ $D_\alpha^I = D_{FKL}$, and in the previous sections we have seen that both $m_{D_{RKL}}$ and $m_{D_{FKL}}$ do not have local minima. Thus, it is very likely that for α sufficiently close to 0 or to 1 the surface of $m_{D_\alpha^I}$ tends to be convex, thus making it easier for the FPI to reach the minimum.

The α -divergences of the II° kind, defined in (39), when applied to pairs of Gaussians is:

$$D_\alpha^{II}(\nu_i \parallel \nu_j) = -\log c_\alpha(\nu_i, \nu_j), \quad (35)$$

with $c_\alpha(\nu_i, \nu_j)$ taking the form (48). As discussed in the Appendix, for $\alpha = 0.5$, D_α^{II} coincides with the *Bhattacharyya distance*. One nice property of this class of α -divergences, is that the fixed-point iteration for the barycenter computation results to be simpler if compared to the divergences of the first kind, mainly because the Chernoff coefficient is cancelled out. The fixed-point iteration derived for the D_α^{II} -barycenter is:

$$\begin{aligned}\hat{\mu}^{k+1} &= \frac{1}{s(\mathbf{w})} \sum_{i=1}^n w_i \bar{\mu}_{i,\nu^k}^\alpha \\ \hat{\Sigma}^{k+1} &= \frac{1}{s(\mathbf{w})} \sum_{i=1}^n w_i (\bar{\Sigma}_{i,\nu^k}^\alpha + (\bar{\mu}_{i,\nu^k}^\alpha - \hat{\mu}^k)(\bar{\mu}_{i,\nu^k}^\alpha - \hat{\mu}^k)^T)\end{aligned}\quad (36)$$

In Fig. 8 the $m_{D_\alpha^{II}}$ surface for $\alpha = 0.5$, which corresponds to m_{D_B} , where D_B is the *Bhattacharyya distance*.

IV. DISCUSSION

In the previous section several fixed-point iterations (FPI) have been reported for different D -measures, but little has been said regarding the initialization, the stopping criteria and convergence. The example (13) we have reported is particularly simple, thus it should not be taken as a way to

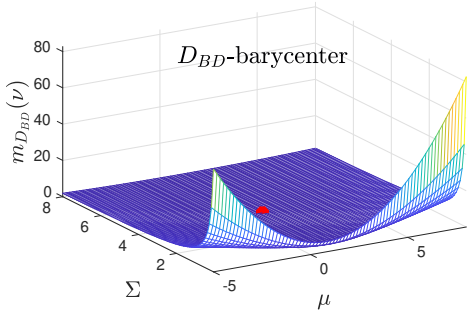


Figure 8. $\hat{\mu}_{D_B} = 1.3148$, $\hat{\Sigma}_{D_B} = 3.8914$

figure out where and when the algorithm will converge, given that the parameter space gets more and more complicated while the dimensionality of the problem increases. The only way to figure out if the barycenter solution is unique for a given D -measure should be by investigating analytically the general case, even if it might be really difficult from several points of view.

If we consider the α -divergences of the second kind, they belong to the Burbea-Rao class [11], for which it is proven that the barycenter exists and it is unique. Thus, we expect the algorithm to always converge; still, the initialization might influence the convergence time. One thing that we empirically observed, is that the Bhattacharyya distance is not too different in the nature from the D_{FKL} . Moreover, even the barycenters appear to be similar. Thus, it might be reasonable to choose as initial guess for the Bhattacharyya barycenters the parameters obtained as the moment-preserving merge (15)–(16) of the components. One interesting link between the Bhattacharyya the Cauchy-Schwarz FPI iterations, (31) and (36), with $\alpha = 0.5$, is that the covariance iterations differ by a factor 2. Thus, it might be reasonable to presume uniqueness for the D_{CS} -barycenters too, although, to the best of our knowledge, there is no proof of that at this moment. For the same reason, one could consider the D_{FKL} -barycenter parameters as initial guess for the D_{CS} -barycenter fixed-point recursion.

The FPI (27) for the D_{W2} -barycenter has been proposed in [5], without any proof of convergence, with the support of successful numerical tests. Regarding the initialization, since the D_{W2} measure is exclusive in the nature, a reasonable initial guess is the D_{RKL} -barycenter parameters, which is an exclusive measure too, and has a closed form solution for the barycenter of a WSG. Nonetheless, a simpler initial guess, which also work well, is $\Sigma_0 = \frac{1}{w} \sum_i w_i \Sigma_i$.

Regarding the D_{SKL} -barycenters, as discussed in [12], they are unique, and an alternative algorithm is proposed to evaluate such quantity; in any case we have decided to stick with the provided algebraic formulation (23) given that it results to be pretty simple to understand and implement. Moreover, the recursion here provided converges really fast $\forall \alpha \in (0, 1)$, even in high dimensional problems.

Regarding the D_α^I -barycenters, we mentioned that for $\alpha \in (0, 1)$ the solution might not be unique. From several tests, there has not been a prevalent heuristic in the choice of the initial guess. What we can say, though, is that particularly

exclusive measures tend to foster the main peaks of the distribution, hence a computationally efficient (quick convergence) way, for instance in the D_{H2} case, might be to consider as initial guess the parameters of the component associated to the highest weight. Nonetheless, given that the main peaks might represent significant local minima, by initializing the recursion on those, the algorithm will probably stick with the corresponding, potentially sub-optimal, solution. Alternatively, one might consider again the D_{FKL} -barycenter, which in general results to be an inclusive solution, thus leaving more chance to converge to a different minimum w.r.t. the ones associated with the main peaks.

The same argumentation can be extended to measures as the Square L2 norm, for which there are present several local minima when seeking the barycenter problem solution.

To conclude this section, the stopping criteria will be discussed. Given that all the fixed-point iteration algorithms converge to a solution with arbitrary accuracy, one should fix a maximum number of allowed iterations and a tolerance on the approximation accuracy. Regarding the former, some algorithms, especially in the D_{H2} or D_{L2} cases, might take many iterations to converge when dealing with high-dimensional problems; for this reason, one might think to either permit a large number of iterations, or allow for smaller accuracy in the resulting approximation. Regarding the tolerance, considering that, in the Gaussian case, we are looking for the mean and the covariance parameters, one could consider to check the accuracy by evaluating the variation in norm between the parameters updates. Otherwise, one could consider the divergence between the barycenter at the previous iteration, and the new one obtained from a recursion step. In both cases, it is important to select the tolerance order of magnitude accordingly.

V. CONCLUSIONS

In this work Fixed-Point Iteration (FPI) algorithms are provided for the computation of barycenters of Weighted Sets of Gaussians (WSG) according to several dissimilarities (D -measures). The barycenter has been defined as the minimizer of an *average dissimilarity function* (ADF). Suitably exploiting the notation and identities provided in Sec. VI-A, we succeeded in obtaining compact formulations of FPIs that solve the minimization problem for a wide set of D -measures. It has been stressed that, depending on the chosen D -measure, the ADF may have local minima or not. To help visualize such cases, the plots of the ADFs of the considered D -measures have been reported for a simple WSG chosen as an example. Initialization issues have been discussed, and the convergence of all the FPI algorithms presented has been successfully tested on a large number of randomly generated WSGs. As a future work, we are planning to try to provide theoretical convergence guarantees.

VI. APPENDIX

The list of divergences (D -measures) used in this paper is reported below (all ratios between pdfs are assumed well

defined):

Kullback-Leibler $D_{KL}(p||q) = \int p(x) \log \frac{p(x)}{q(x)} dx,$

Jeffreys (symm-KL) $D_J(p||q) = \frac{1}{2}(D_{KL}(p||q) + D_{KL}(q||p))$
 $= \frac{1}{2} \int (p(x) - q(x)) \log \frac{p(x)}{q(x)} dx,$

Skew Jeffreys $D_J^\alpha(p||q) = (1 - \alpha)D_{KL}(p||q) + \alpha D_{KL}(q||p),$

Square L2 norm
aka Integral Square Error (ISE) $D_{L2}(p||q) = \int (p(x) - q(x))^2 dx,$

Cauchy-Schwarz $D_{CS}(p||q) = -\log \left(\frac{\int p(x)q(x)dx}{\sqrt{(\int p^2(x)dx)(\int q^2(x)dx)}} \right)$

Bhattacharyya $D_B(p||q) = -\log \int \sqrt{p(x)q(x)} dx,$

Square Hellinger $D_{H2}(p||q) = \frac{1}{2} \int (\sqrt{p(x)} - \sqrt{q(x)})^2 dx$
 $= 1 - \int \sqrt{p(x)q(x)} dx,$

Pearson χ^2 $D_P(p||q) = \frac{1}{2} \left(\int \frac{q(x)^2}{p(x)} dx - 1 \right),$

Neyman χ^2 $D_N(p||q) = \frac{1}{2} \left(\int \frac{p(x)^2}{q(x)} dx - 1 \right).$

Square
2-Wasserstein $D_{W2}(p||q) = \inf_{\pi \in \mathcal{P}_2} \iint \|x - y\|^2 \pi(x, y) dx dy$

where \mathcal{P}_2 is the set of all pdfs in $\mathbb{R}^d \times \mathbb{R}^d$ that have $p(x)$ and $q(y)$ as marginals and finite second order moments.

α -divergences

The Chernoff α -coefficient $c_\alpha(p, q)$, $\alpha \in (-\infty, \infty)$, defined as

$$c_\alpha(p, q) = \int p^\alpha(x) q^{1-\alpha}(x) dx \quad (37)$$

allows to define two families of divergences: α -divergences of the I° and of then II° kind:

I° kind α -div $D_\alpha^I(p||q) = \frac{1}{\alpha(1-\alpha)}(1 - c_\alpha(p, q)), \quad (38)$

II° kind α -div $D_\alpha^{II}(p||q) = -\log c_\alpha(p, q). \quad (39)$

For some values of α , the α -divergences of the I° kind coincide with some of the previously listed divergences:

$$\begin{aligned} D_\alpha^I(p||q)|_{\alpha=-1} &= D_P(p||q) && \text{Pearson } \chi^2 \\ \lim_{\alpha \rightarrow 0} D_\alpha^I(p||q) &= D_{KL}(q||p) && \text{Reverse KL} \\ D_\alpha^I(p||q)|_{\alpha=0.5} &= 4D_{H2}(p||q) && \text{Square Hellinger} \\ \lim_{\alpha \rightarrow 1} D_\alpha^I(p||q) &= D_{KL}(p||q) && \text{Forward KL} \\ D_\alpha^I(p||q)|_{\alpha=2} &= D_N(p||q) && \text{Neyman } \chi^2 \end{aligned} \quad (40)$$

For $\alpha = 0.5$, $c_\alpha(p, q)$ coincides with the Bhattacharyya coefficient [11] and the corresponding α -divergence of the II° kind coincides with the Bhattacharyya divergence.

A. Some useful formulas

The *cross-likeness* $J_{i,j}$ between two Gaussians $\nu_i = \mathcal{N}(x|\mu_i, \Sigma_i)$ and $\nu_j = \mathcal{N}(x|\mu_j, \Sigma_j)$ is defined in [9] as

$$J_{i,j} = \int \nu_i(x) \cdot \nu_j(x) dx = \mathcal{N}(\mu_i|\mu_j, \Sigma_i + \Sigma_j). \quad (41)$$

The *self-likeness* of a Gaussian ν_i is

$$J_{i,i} = \int \nu_i^2(x) dx = \mathcal{N}(\mu_i|\mu_i, 2\Sigma_i) = |4\pi\Sigma_i|^{-\frac{1}{2}}. \quad (42)$$

If ν is without subscript, then the self-likeness is written $J_{\nu,\nu}$, so that $J_{\nu,\nu} = \mathcal{N}(0|0, 2\Sigma)$, and the cross-likeness between ν_i and ν is written as $J_{i,\nu}$. The following hold true

$$\nu_i(x) \cdot \nu(x) = J_{i,\nu} \mathcal{N}(x|\bar{\mu}_{i,\nu}, \bar{\Sigma}_{i,\nu}) \quad (43)$$

where $\bar{\mu}_{i,\nu} = (\Sigma_i^{-1} + \Sigma^{-1})^{-1}(\Sigma_i^{-1}\mu_i + \Sigma^{-1}\mu)$
 $\bar{\Sigma}_{i,\nu} = (\Sigma_i^{-1} + \Sigma^{-1})^{-1}$ (44)

$$\nu^2(x) = J_{\nu,\nu} \mathcal{N}(x|\mu, \frac{1}{2}\Sigma) = \frac{1}{\sqrt{|4\pi\Sigma|}} \mathcal{N}(x|\mu, \frac{1}{2}\Sigma). \quad (45)$$

For any $\alpha \in (0, 1)$ we have:

$$\begin{aligned} \nu^\alpha &= \frac{(2\pi)^{\frac{d}{2}(1-\alpha)} |\Sigma|^{\frac{1-\alpha}{2}}}{\alpha^{\frac{d}{2}}} \mathcal{N}(x|\mu, \frac{1}{\alpha}\Sigma), \\ \nu^{1-\alpha} &= \frac{(2\pi)^{\frac{d}{2}\alpha} |\Sigma|^{\frac{\alpha}{2}}}{(1-\alpha)^{\frac{d}{2}}} \mathcal{N}(x|\mu, \frac{1}{1-\alpha}\Sigma). \end{aligned} \quad (46)$$

The Chernoff α -coefficient (37) between ν_i and ν_j is

$$c_\alpha(\nu_i, \nu_j) = \left(\frac{|\bar{\Sigma}_{i,j}^\alpha|}{|\Sigma_i|^\alpha |\Sigma_j|^{1-\alpha}} \right)^{\frac{1}{2}} e^{-\frac{1}{2}(\mu_i - \mu_j)^T (\bar{\Sigma}_{i,j}^\alpha)^{-1} (\mu_i - \mu_j)} \quad (47)$$

so that $\nu_i^\alpha \cdot \nu^{1-\alpha} = c_\alpha(\nu_i, \nu) \cdot \mathcal{N}(x|\bar{\mu}_{i,\nu}^\alpha, \bar{\Sigma}_{i,\nu}^\alpha), \quad (48)$

where $\bar{\Sigma}_{i,\nu}^\alpha = (\alpha\Sigma_i^{-1} + (1-\alpha)\Sigma^{-1})^{-1},$
 $\bar{\mu}_{i,\nu}^\alpha = \bar{\Sigma}_{i,\nu}^\alpha (\alpha\Sigma_i^{-1}\mu_i + (1-\alpha)\Sigma^{-1}\mu).$ (49)

By exploiting (11), the derivatives of ν^α and $\nu^{1-\alpha}$ w.r.t. the parameters (μ, Σ^{-1}) can be obtained in a straightforward manner.

Similarly, using (11) the derivatives of the cross-likeness $J_{i,\nu}$, between ν_i and ν and of the self-likeness $J_{\nu,\nu}$, with respect to the parameters (μ, Σ^{-1}) of ν can be obtained:

$$\begin{aligned} \frac{\partial J_{i,\nu}}{\partial \mu} &= \Sigma^{-1}(\bar{\mu}_{i,\nu} - \mu) J_{i,\nu}, & \frac{\partial J_{\nu,\nu}}{\partial \mu} &= 0 \\ \frac{\partial J_{i,\nu}}{\partial \Sigma^{-1}} &= \frac{1}{2}(\Sigma - (\bar{\Sigma}_{i,\nu} + (\bar{\mu}_{i,\nu} - \mu)(\bar{\mu}_{i,\nu} - \mu)^T)) J_{i,\nu} \\ \frac{\partial J_{\nu,\nu}}{\partial \Sigma^{-1}} &= \frac{1}{2} J_{\nu,\nu} \Sigma \end{aligned} \quad (50)$$

Analogous derivatives can be obtained for the Chernoff α -coefficient, omitted due to their cumbersome forms.

REFERENCES

- [1] Pedro C. Álvarez-Esteban, E. del Barrio, J.A. Cuesta-Albertos, C. Matrán, *A fixed-point approach to barycenters in Wasserstein space*, J. of Math. Analysis and Applications, Vol. 441, no. 2, pp. 744-762, 2016.
- [2] A. Assa and K.N. Plataniotis, *Wasserstein-Distance-Based Gaussian Mixture Reduction*, in IEEE Signal Proc. Letters, vol. 25, no. 10, pp. 1465–1469, Oct. 2018.
- [3] G. Battistelli and L. Chisci, *Kullback–Leibler average, consensus on probability densities, and distributed state estimation with guaranteed stability*, Automatica, vol. 50, no. 3, pp. 707–718, 2014.
- [4] N. Bouguila, W. Fan (Eds.), *Mixture Models and Applications*, Unsupervised and Semi-Supervised Learning series, Springer, 2020.
- [5] Y. Chen, T.T. Georgiou and A. Tannenbaum, *Optimal Transport for Gaussian Mixture Models*, IEEE Access, vol. 7, pp. 6269-6278, 2019.
- [6] S. Clatici, E. Chien, J. Solomon, *Stochastic Wasserstein Barycenters*, proc. of the 35th Int. Conf. on Machine Learning, Stockholm, Sweden, 2018.
- [7] A. D’Ortenzio and C. Manes, *Composite Transportation Dissimilarity in Consistent Gaussian Mixture Reduction*, 2021 IEEE 24th Int. Conf. on Information Fusion (FUSION), 2021, pp. 1-8.
- [8] A. D’Ortenzio, C. Manes, *Consistency issues in Gaussian Mixture Models reduction algorithms*, arXiv:2104.12586 [stat.ML], 2021
- [9] A. D’Ortenzio and C. Manes, *Likeness-Based dissimilarity measures for Gaussian Mixture Reduction and Data Fusion*, 2021 IEEE 24th Int. Conf. on Information Fusion (FUSION), 2021, pp. 1-8.
- [10] S. Kullback, R.A. Leibler, *On Information and Sufficiency*, The Ann. of Math. Statistics, vol. 22, no. 1, pp. 79–86, 1951.
- [11] F. Nielsen and S. Boltz, *The Burbea-Rao and Bhattacharyya Centroids*, in IEEE Trans. on Information Theory, vol. 57, no. 8, pp. 5455-5466, Aug. 2011.
- [12] F. Nielsen and R. Nock, *Sided and Symmetrized Bregman Centroids*, in IEEE Trans. on Information Theory, vol. 55, no. 6, pp. 2882-2904, June 2009.
- [13] A.R. Runnalls, *Kullback-Leibler approach to Gaussian mixture reduction*, IEEE Trans. Aerosp. Electron. Sys., V. 43, N. 3, pp. 989–999, 2007.